Multiscale - Patient-Specific Artery and Atherogenesis Models

P. Siogkas, A. Sakellarios, T. P. Exarchos, *Member, IEEE*, L. Athanasiou, E. Karvounis, K. Stefanou, E. Fotiou, D. I. Fotiadis*, *Senior Member, IEEE*, K. K. Naka, L. K. Michalis, N. Filipovic, and O. Parodi

***Abstract*—In this work, we present a platform for the development of multiscale patient-specific artery and atherogenesis models. The platform, called ARTool, integrates technologies of 3-D image reconstruction from various image modalities, blood flow and biological models of mass transfer, plaque characterization, and plaque growth. Patient images are acquired for the development of the 3-D model of the patient specific arteries. Then, blood flow is modeled within the arterial models for the calculation of the wall shear stress distribution (WSS). WSS is combined with other patient-specific parameters for the development of the plaque progression models. Real-time simulation can be performed for same cases in grid environment. The platform is evaluated using both animal and human data.**

***Index Terms*—3-D image reconstruction, atherosclerosis, blood flow dynamics, plaque progression.**

I. Introduction

CARDIOVASCULAR diseases are the leading cause of death in western societies. More specifically, the most prevalent of cardiovascular diseases is considered to be atherosclerosis. Atherosclerosis is an inflammatory disease, which is described by the accumulation of cell debri, fatty ingredients such as cholesterol, fibrous tissue, calcium, and white blood cells on the arterial walls. This biological process results to the formation of atheromatic plaque and the deterioration of the elasticity of the arterial wall. Atheromatic plaque is increased over time and causes the narrowing of arteries, obstructing thus blood flow. Plaque progression is directly affected by mechanical, biochemical, and biological factors. Researchers made some early attempts to understand this process with the use of *in vitro* experiments. Recent advances in both computational fluid dynamics (CFD) and in medical imaging techniques have contributed to the modeling of the formation and progression of atheromatic plaque. Data obtained by imaging modalities, such as intravascular ultrasound (IVUS) and angiography, magnetic resonance imaging (MRI), and computed tomography (CT) are considered to be fundamental in arterial modeling. Bourantas *et al*. [1] used data fusion of IVUS and angiography images to reconstruct coronary arteries in 3-D. Yang *et al*. [2] utilized CT angiography images to reconstruct the left and right coronary arteries of human subjects. Tang *et al*. [3] generated a 3-D model based on MR images incorporating multicomponent plaque formations. In a later study by the same group [4], 3-D carotid models reconstructed from MRI data were used to correlate carotid plaque progression with flow shear stress. MRI data were used by Steinman *et al.* [5] for the reconstruction of carotid artery bifurcations. The resulting 3-D models of the aforementioned methods have been used to simulate blood flow and draw conclusions about the effect of shear stress distribution on plaque progression. The endothelial function is primarily affected by blood flow, which, in turn, promotes atherosclerosis. Curvatures and bifurcations in the arterial tree create complex flows and are consequently more prone to plaque development. Compliant unrealistic arterial models were used by Canic *et al.* [6] to perform blood flow simulations. Blood flow was modeled using the Navier – Stokes equations whereas the material of the arterial wall was considered as linear viscoelastic. The mechanical properties of the arterial wall are an unresolved issue due to the lack of *in vivo* data. Several models have been used in literature to describe the arterial wall. In [7] a comparative study on the modeling of arterial mechanics is presented.

Regarding models for mass transport and plaque progression, several studies have been proposed to model the mass transport and endothelial permeability in arteries. The most common used conditions for the endothelial permeability are the Kedem-Katchalsky equations, which describe the permeability in biological membranes. Complex transport models in arteries consider the arterial wall as multilayer, consisting of more than one layer [8]. These models are more realistic because they represent the arterial wall constituting from the endothelium, the intima, the media, and the adventitia.

In the current work, we present a platform for the development of multiscale patient specific atherogenesis models, called

Manuscript received April 1, 2011; revised June 23, 2011; accepted August 1, 2011. Date of publication August 15, 2011; date of current version November 18, 2011. This work was funded in part by the EC Project ARTreat: Multilevel patient-specific artery and atherogenesis model for outcome prediction, decision support treatment, and virtual hand-on training, FP7 – 224297. *Asterisk indicates corresponding author.*

P. Siogkas, A. Sakellarios, T. P. Exarchos, E. Karvounis, and K. Stefanou are with the Foundation of Research and Technology Hellas - Biomedical Research Institute, Ioannina, Greece (e-mail: ansakel@cc.uoi.gr, psiogkas@cc.uoi.gr exarchos@cc.uoi.gr, ekarvuni@cc.uoi.gr, kstefan@cc.uoi.gr).

L. Athanasiou is with the Unit of Medical Technology and Intelligent Information Systems, Department of Material Science and Engineering, University of Ioannina, Ioannina, Greece (e-mail: lmathanas@cc.uoi.gr).

E. Fotiou is with the d.d. Synergy Hellas, Athens, Greece (e-mail: v_fotiou@ddsynergy.gr).

*D. I. Fotiadis is with the Foundation of Research and Technology Hellas -Biomedical Research Institute, Ioannina, Greece (e-mail: fotiadis@cc.uoi.gr).

K. K. Naka and L. K. Michalis are with the Medical School, University of Ioannina, Ioannina, Greece (e-mail: anaka@cc.uoi.gr, lmihalis@cc.uoi.gr).

N. Filipovic is with the University of Kragujevac, Kragujevac, Serbia (e-mail: fica@kg.ac.rs).

O. Parodi is with the Institute of Clinical Physiology, National Research Council, Pisa, Italy (e-mail: oberpar@tin.it).

Color versions of one or more of the figures in this paper are available online at http://ieeexplore.ieee.org.

Digital Object Identifier 10.1109/TBME.2011.2164919

ARTool. The methodology integrates three levels involved in the atherogenesis procedure, that is the anatomical model of the arterial tree, the blood flow model and the molecular/cell model of the arterial wall/blood composition and the biological mechanism involved in the generation and growth of atherosclerotic plaque.

II. Methods

A. 3-D Image Reconstruction

The 3-D image reconstruction software that is used within ARTool has been developed based on recent research studies. All algorithms have been previously validated and proven to be effective.

The platform is able to process images from various imaging modalities. More specifically, IVUS and bi-plane angiography are used for the reconstruction of coronary arterial segments [1]. Two-end diastolic angiographic images are used to predict the catheter path. The artery path is approximated using cubic B – Splines and the catheter path is created by the intersection of two splines. IVUS frames are collected at the peak of the R wave.

MRI is used for the reconstruction of carotid arteries [9]. Active contours with gradient vector flow snakes are used along with edge-detection techniques for the estimation of the lumen and outer wall border in time of flight (TOF) and T_1 weighted (T_1W) MR images, respectively. The frame where the bifurcation appears is detected and an interpolation approach is used for the estimation of the bifurcation.

CT reconstruction is based on [10]. In the proposed approach, the segmentation algorithm traverses the 3-D volume twice, which is the minimum number of iterations in order to segment objects in a 3-D volume. Details for the MRI and CT reconstruction methods can be found in [11].

B. Blood Flow and Biological Process Modeling

ARTool offers the capability to perform blood flow simulations under the assumption of either rigid or deformable walls regarding the 3-D models, using the finite element method (FEM). Fluid structure interaction (FSI) models are implemented using the loose coupling method to solve the appropriate equations. The arterial walls are considered to be either elastic or hyperelastic and their distal ends are fixed to prevent motion of those regions.

Wall shear stress (WSS) as well as low density lipoprotein (LDL) distribution are calculated in order to reveal areas of high risk of plaque initiation or progression. Fluid shear stress in our model is used for the plaque initiation and position at the wall for higher LDL penetration. Blood flow in the lumen domain, which is considerd as a 3-D fluid flow, is modeled by the Navier-Strokes equations, together with the continuity equation for incompressible fluid

$$-\mu\nabla^2\mathbf{u}_l + \rho\left(\mathbf{u}_l\cdot\nabla\right)\mathbf{u}_l + \nabla p_l = 0 \tag{1}$$

$$\nabla\cdot\mathbf{u}_l = 0 \tag{2}$$

where $\mathbf{u}_l$ is the blood velocity in lumen, p_l is the pressure, μ is the dynamic viscosity of blood, and ρ is the blood density [18].

Mass transfer in the lumen is coupled with the blood flow and is modeled by a convection-diffusion equation, in the fluid domain

$$\nabla\cdot\left(-D_l\nabla c_l + c_l\mathbf{u}_l\right) = 0 \tag{3}$$

where c_l is the solute concentration in the blood and D_l is the solute diffusivity in the lumen. Mass transfer in the arterial wall is coupled to the transmural flow and modeled by a convection-diffusion-reaction equation as follows:

$$\nabla\cdot\left(-D_w\nabla c_w + kc_w u_w\right) = r_w c_w \tag{4}$$

where c_w is the solute concentration and D_w is the solute diffusivity in the arterial wall; u_w is the blood velocity in the wall, K is the solute lag coefficient, and r_w is the consumption rate constant. The LDL transport in the lumen and in the vessel wall are coupled by the Kedem-Katchalsky equations

$$J_v = L_p\left(\Delta p - \sigma_d\Delta\pi\right) \tag{5}$$

$$J_s = P\Delta c + \left(1-\sigma_f\right)J_v\bar{c} \tag{6}$$

where L_p is the hydraulic conductivity of the endothelium; Δc is the solute concentration difference, Δp is the pressure drop, and $\Delta\pi$ is the oncotic pressure difference all across the endothelium; σ_d is the osmotic reflection coefficient, σ_f is the solvent reflection coefficient, P is the solute endothelial permeability, and $\bar{c}$ is the mean endothelial concentration. The first term in the Kedem-Katchalsky equations ($P\,\Delta c$) of the right hand side (6) defines the diffusive flux across the endothelium, while the second term $\left(1-\sigma_f\right)J_v\bar{c}$ defines the convective flux. Only the oncotic pressure difference $\Delta\pi$ is neglected in our simulations due to the decoupling of the fluid dynamics from solute dynamics. The above governing equations are transformed into an FE system of incremental-iterative equations and solved over time steps [12].

The atherosclerotic process starts with the accumulation of LDL in the intima, where part of them are oxidized and become pathological. In order to remove the oxidized particles, circulating immune cells (e.g., monocytes) are recruited. Once in the intima, the monocytes differentiate and become macrophages that phagocyte the oxidized LDL. Fatty macrophages then transform into foam cells. Foam cells are responsible for the growth of a subendothelial plaque which eventually emerges in the artery lumen. The model is a coupled fluid-intima model, since new mass tissue is generated from the foam cells and we have the intima volume increasing, which is fully coupled with the lumen domain.

The inflammatory process (transformation of macrophages into foam cells) is modeled using three additional reaction-diffusion partial differential equations

$$\partial_t Ox = d_1\Delta Ox - k_1 Ox\cdot M \tag{7}$$

$$\partial_t M + \mathrm{div}(v_w M) = d_2\Delta M - k_1 Ox\cdot M + S/(1-S) \tag{8}$$

$$\partial_t S = d_3\Delta S - \lambda S + k_1 Ox\cdot M + \gamma(Ox - Ox^{\mathrm{thr}}) \tag{9}$$

where Ox is the oxidized LDL in the wall, M and S are concentrations of macrophages and cytokines, respectively, in the intima; d_1,d_2,d_3 are the corresponding diffusion coefficients; λ and γ are the degradation, and LDL oxidized detection coefficients; and v_w is the inflammatory velocity of plaque growth, which satisfies Darcy's law and the incompressibility continuity equation

$$v_w - \nabla \cdot (p_w) = 0 \tag{10}$$

$$\nabla v_w = 0 \tag{11}$$

in the wall domain. p_w is the pressure in the arterial wall.

In order to follow the changes of the vessel wall geometry during plaque growth, a 3-D mesh moving algorithm, the arbitrary lagrangian eulerian (ALE) is applied. ALE formulation is developed for mesh moving and changing of the structural domain due to intima volume thickness and fluid domain reduction in time. In this way, we included both structural and fluid domain. Macro growth is connected through (10) and (11) and the inflammatory velocity v_w of the plaque growing from (7)–(9). Two time points were examined, one at the baseline and the other after a period of two months of high fat diet.

C. Plaque Characterization

ARTool includes also an automated plaque characterization application using three image modalities, IVUS, MRI, and CT. Concerning the plaque characterization module using IVUS images, a hybrid approach is used, that is based on image filtering and random forests. The classification scheme includes soft plaques (lipid), hard plaques (calcium and fibrotic), and hard calcified (calcium) plaques. The characterization of plaque using MRI was based on an image processing algorithm which uses as input three different contrast weightings of MRI: T_1, T_2, and Proton Density (PD). The algorithm classifies: fibrous tissue, lipid core, hemorrhages, and calcifications. Finally, the method developed to characterize plaque formations using CT images includes the detection and characterization of calcium formations. The image processing technique that was developed is based on the fact that calcium appears brighter than the lumen in the CT.

III. Results

The platform can be used for the visualization, assessment, and prediction of the atherosclerotic plaque development. The 3-D reconstruction module gives the capability for fast and accurate reconstruction of arterial segments and trees. The algorithms are validated using annotated datasets by expert physicians. The mean error of the lumen and media-adventitia area is $-0.63 \pm 8.71\%$ and $-2.09 \pm 8.61\%$, respectively, in the IVUS and angiography reconstruction. In the case of the carotid artery reconstruction using MRI the mean error is $-3.21 \pm 6.39\%$ and $1.92 \pm 5.88\%$ for the lumen and outer vessel wall, respectively. In the case of CT reconstruction, the MICCAI evaluation framework [10] was employed, by measuring the number of correctly segmented arteries. The accuracy obtained is 84.1%.

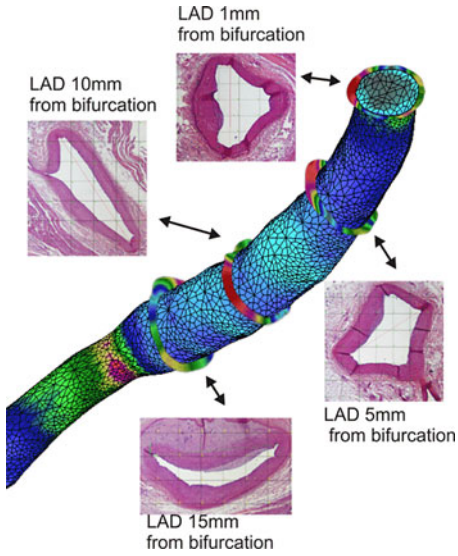

Fig. 1. Matching IVUS and histological cross-sectional geometry. Shear stress distribution is shown along the internal arterial wall.

Fig. 2. Computer reconstruction of a cross-section of LAD at 15 mm after bifurcation (left panel), with computed concentration of macrophages [mg/ml] (middle panel); histological analysis (right panel) after two months of the high fat diet.

The reconstructed arterial models are used for the simulation of blood flow. FEM is used for calculating blood flow velocities and WSS, which are assessed to have a significant role in plaque development. Validation in blood flow modeling is based on Doppler or MRI data for coronary and carotid arteries, respectively. The mean error is 4%.

Regarding the plaque progression models, we used experimental data from pigs submitted to a high cholesterol diet for two months. The lumen and the outer wall of the arteries were reconstructed and then, matching of histological data and IVUS slices was performed, as it is shown in Fig. 1.

The left arterior descending (LAD) was selected for this analysis. The process of matching with IVUS images was achieved by 2-D modeling of tissue deformation for a number of cross-sections recorded by histological analysis (four cross-sections are shown in Fig. 1); those cross-sections are deformed until the internal lumen circumferential lengths in IVUS images are reached. Macrophages distribution shown in Fig. 2 corresponds to the low WSS zone at 15 mm below LAD bifurcation from the left circumflex artery, where the largest plaque formation was found. The volume of plaque was obtained by matching IVUS segmentation cross-section and histological intima thickness at

TABLE I
VALUES FOR THE ANIMAL EXPERIMENTS

Lumen	Intima	Inflammation
ρ=1000 kg/m^3		d_1=10^{-8} m^2/s
μ = 0.035 [P]		d_2=10^{-10} m^2/s
D_l = 3.2x10^{-11} m^2/s	D_w = 1.3x10^{-11} m^2/s	d_3=10^{-8} m^2/s
Umax=0.4m/s	r_w = -2.6x10^{-4}	k1=20^{-6} m^3/kg s
Pout=100mmHg	Pmed=100mmHg	λ=25 s^{-1}
Co=3.0x10^{-12} kg/m^3		γ = 1 s^{-1}

the same radial position. After 3-D reconstruction of plaque geometry, the inflammatory velocity v_w from (10) and (11) was fitted using nonlinear least square analysis for two time points, baseline, and after two months' high fat diet. It was assumed that the intimal thickness corresponds to the geometrical volume change in time. The diffusion coefficients d_1, d_2, d_3 for oxidized LDL, macrophages, and cytokines as well as degradation and LDL oxidized detection coefficients λ and γ, coefficient k_1 are fitted using least square analysis [13]. The threshold for oxidized LDL and cytokines Ox^{thr} was assumed to be zero. Other material parameters for the lumen are taken from literature and boundary conditions for flow and pressure are averaged from experimental measurements for a specific pig. The fitted numerical parameters are given in Table I.

Regarding the results of the plaque characterization, the plaque characterization application using IVUS was tested using 40 annotated IVUS images, and resulted to 87.81% accuracy for hard calcified plaque formations, 84.05% for soft plaque formations, and 88.32% accuracy for the hard noncalcified plaque formations. The designed algorithm for characterizing the plaque using MR images, was tested using 521 MR images (from three sequences) annotated by experts. Statistical analysis for the lipid component in terms of Cohen's k and Pearson correlation coefficient r resulted to $k = 0.68$, $r = 0.95$. Finally, CT plaque characterization method was compared with expert annotation. The algorithm showed high correlation and accuracy. More specifically, plaque formations from ten patients were annotated by experts. Concerning the plaque formations in coronary arteries, statistical analysis resulted to $k = 0.74$, $r = 0.97$ while for the carotid arteries the analysis resulted to $k = 0.96$, $r = 0.98$.

IV. DISCUSSION

A multiscale model for the biological process of plaque formation and progression is presented. The model includes the 3-D reconstructed arterial model, the blood flow, the WSS distribution, the molecular/cell model of the arterial wall/blood composition, and the biological mechanism involved in the generation and growth of atherosclerotic plaque. The governing partial differential equations for plaque formation rely on the mass balance and Darcy's law in the domain of plaque development; the Navier-Stokes equations and diffusion equations are used for the LDL transport within the arterial lumen; the transport-diffusion-reaction equations are employed for the transmural mass transport, including the Kedem-Katchalsky equations to couple the transmural and transport within the lumen. The wall permeability was assumed to be a function of the wall shear stress with lower permeability at low and oscillatory shear stress.

We describe the inflammatory process using reaction-diffusion equations. Our model starts with passive penetration of LDL in particular areas of the intima. We assume that once in the intima, LDL is immediately oxidized. When the oxidized LDL exceeds a threshold there is recruitment of monocytes. The incoming monocytes immediately differentiate into macrophages. Transformation of macrophages into foam cells contribute to the recruitment of new monocytes. This yields the secretion of a proinflammatory signal (cytokines), self-support inflammatory reaction. Newly formed foam cells are responsible for the local volume increase. Under a local incompressibility assumption, when foam cells are created, the intima volume is locally increasing. Volume change of the wall affects the fluid lumen domain, which means that fully coupling is achieved. The specific numerical procedures using ALE were developed for this purpose. Our approach is concentrated on the process on plaque initiation and intimal thickening.

Smooth muscle cells proliferation was not taken into account in this model and will be investigated in a future study. Moreover, we have not taken into account deformation and stress inside the arterial wall, which is very important for the plaque rupture and smooth muscle proliferation for plaque growing. Another limitation of the platform is that, currently, plaque characterization is performed in 2-D images; however, we are in the process of connecting the 2-D characterized images in order to create 3-D volumes of the plaque. Then, blood flow modeling and the subsequent plaque progression will become much more realistic.

We examined experimental data obtained for the LAD artery of a pig after two months' high fat diet in order to determine material parameters of the model. The matching between computed plaque location and progression in time with experimental observations demonstrate a potential benefit for future prediction of this vascular decease.

REFERENCES

[1] C. Bourantas, F. Kalatzis, M. Papafaklis, D. Fotiadis, A. Tweddel, I. Kourtis, C. Katsouras, and L. Michalis, "ANGIOCARE: An automated system for fast three- dimensional coronary reconstruction by integrating angiographic and intracoronary ultrasound data," *Cath. Cardio. Interv.*, vol. 72, pp. 166–175, 2008.

[2] Y. Yang, A. Tannenbaum, D. Giddens, and A. Stillman, "Automatic segmentation of coronary arteries using bayesian driven implicit surfaces," in *Proc. 4th IEEE Int. Symp. Biomed. Imag.*, 2007, pp. 189–192, art. no. 4193254.

[3] D. Tang, C. Yang, J. Zheng, P. K. Woodard, G. A. Sicard, J. E. Saffitz, and C. Yuan, "3D MRI-based multicomponent FSI models for atherosclerotic plaques," *Ann. Biomed. Eng.*, vol. 32, pp. 947–960, 2004.

[4] C. Yang, G. Canton, C. Yuan, M. Ferguson, T. S. Hatsukami, and D. Tang, "Advanced human carotid plaque progression correlates positively with flow shear stress using follow-up scan data: An *in vivo* MRI multi-patient 3D FSI study," *J. Biomechanics*, vol. 43, pp. 2530–2538, 2010.

[5] D. Steinman, J. Thomas, H. M. Ladak, J. S. Milner, B. K. Rutt, and J. D. Spence, "Reconstruction of carotid bifurcation hemodynamics and wall thickness using computational fluid dynamics and MRI," *Magn. Reson. Med.*, vol. 47, pp. 149–159, 2002.

[6] S. Čanić, C. Hartley, D. Rosenstrauch, J. Tambača, G. Guidoboni, and A. Mikelić, "Bloof flow in compliant arteries: An effective viscoelastic reduced model, numerics and experimental validation," *Ann. Biom. Eng.*, vol. 34, pp. 575–592, 2006.

[7] G. Holzapfel, T. Gasser, and R. Ogden, "A new constitutive framework for arterial wall mechanics and a comparative study of material models," *J. Elasticity*, vol. 61, pp. 1–48, 2000.

[8] N. Yang and K. Vafai, "Modeling of low-density lipoprotein (LDL) transport in the artery-effects of hypertension," *Int. J. Heat Mass Transfer*, vol. 49, pp. 850–867, 2006.

[9] D. Barratt, B. Ariff, K. Humphries, S. Thom, and A. Hughes, "Reconstruction and quantification of the carotid artery bifurcation from 3-D ultrasound images," *IEEE Trans. Med. Imag.*, vol. 23, no. 5, pp. 567–583, May 2004.

[10] M. Schaap, C. T. Metz, T. van Walsum, A. G. van der Giessen, A. C. Weustink, N. R. Mollet, C. Bauer, H. Bogunović, C. Castro, X. Deng, E. Dikici, T. O'Donnell, M. Frenay, O. Friman, M. H. Hoyos, P. H. Kitslaar, K. Krissian, C. Kühnel, M. A. Luengo-Oroz, M. Orkisz, O. Smedby, M. Styner, A. Szymczak, H. Tek, C. Wang, S. K. Warfield, S. Zambal, Y. Zhang, G. P. Krestin, and W. J. Niessen, "Standardized evaluation methodology and reference database for evaluating coronary artery centerline extraction algorithms," *Med. Image Anal.*, vol. 13, pp. 701–714, 2009.

[11] A. I. Sakellarios, V. D. Tsakanikas, N. Filipovic, L. K. Michalis, D. I. Fotiadis, and C. V. Bourantas, "ARTOOL: A platform for atherosclerosis multilevel modeling," in *Proc. Second South-East Eur. Conf. Comput. Mechanics*, Greece, 2009.

[12] M. Kojic, N. Filipovic, B. Stojanovic, and N. Kojic, *Computer Modeling in Bioengineering: Thoretical Background, Examples and Software*. Chichester, England: John Wiley and Sons, 2008.

[13] G. Chavent, *Nonlinear Least Squares for Inverse Problems, Theoretical Foundations and Step-by-Step Guide for Applications*. New York: Springer, 2010.